Published in "Hippocampus, 2010
doi:10.1002/hipo.20730"
which should be cited to refer to this work.

Developmental Regulation of Gene Expression and Astrocytic Processes May Explain Selective Hippocampal Vulnerability

Pierre Lavenex,[1,2,3]* Steven G. Sugden,[1,2] Ryan R. Davis,[2,4] Jeffrey P. Gregg,[2,4] and Pamela Banta Lavenex[1,2,3]

ABSTRACT: The hippocampus plays a central role in the brain network that is essential for memory function. Paradoxically, the hippocampus is also the brain structure that is most sensitive to hypoxic-ischemic episodes. Here, we show that the expression of genes associated with glycolysis and glutamate metabolism in astrocytes and the coverage of excitatory synapses by astrocytic processes undergo significant decreases in the CA1 field of the monkey hippocampus during postnatal development. Given the established role of astrocytes in the regulation of glutamate concentration in the synaptic cleft, our findings suggest that a developmental decrease in astrocytic processes could underlie the selective vulnerability of CA1 during hypoxic-ischemic episodes in adulthood, its decreased susceptibility to febrile seizures with age, as well as contribute to the emergence of selective, adultlike memory function. © 2009 Wiley-Liss, Inc.

KEY WORDS: Hippocampus; amnesia; hypoxia; ischemia; seizure; fever; epilepsy

INTRODUCTION

The hippocampal formation, a group of cortical regions located in the medial temporal lobe, is essential for memory function and damage to the hippocampus results in amnesia (Milner et al., 1998; Amaral and Lavenex, 2007; Morris, 2007). Paradoxically, the CA1 field of the hippocampus is also the brain structure most sensitive to hypoxic-ischemic events in adulthood (Sommer, 1880; Spielmeyer, 1925; Zola-Morgan et al., 1986; Kass and Lipton, 1989; Banta Lavenex et al., 2006; Andersen et al., 2007). Many researchers therefore focus on this brain region in order to study the cellular and molecular mechanisms of brain damage induced by hypoxic-ischemic events (Pearson et al., 2001; Jensen, 2002; Yin et al., 2002; Krebs et al., 2003; Galeffi et al., 2004; Giffard et al., 2004; Kuan et al., 2004; Holopainen, 2005; Stork and Li, 2006). To date, however, the neurobiological basis for the increased vulnerability of CA1, when compared with other brain regions, is unknown (Lein et al., 2004; Nedergaard and Dirnagl, 2005; Andersen et al., 2007).

Previous studies have examined the molecular characteristics of principal cell populations within the hippocampal formation (Lein et al., 2004; Ginsberg and Che, 2005). Lein and colleagues (2004) used DNA microarray technology and high-throughput in situ hybridization to define the molecular signatures of the dentate gyrus (DG), CA3, and CA1 regions of 10- to 11-week-old C57BL/6 male mice. They identified genes relatively enriched in these different regions and selected a number of these genes whose expression was restricted to neurons, to determine unique signatures of adult neurons in distinct hippocampal regions. Ginsberg and Che (2005) focused their analysis on the gene-expression profiles of pyramidal neurons within the CA3 and CA1 regions of 62–92-yr-old humans. They used a custom-designed cDNA microarray platform representing 125 preselected human genes, including cytoskeletal elements ($n = 12$), glutamate receptors, transporters, and interacting proteins ($n = 28$), and a number of other related transcripts. They found a number of genes to be differentially expressed in CA3 versus CA1 pyramidal neurons. Some glutamatergic receptors (GRIK1, GRIN1, and GRIN2B) and some GABAergic receptors (GABRA1 and GABRA2) were more highly expressed in CA1, whereas other glutamatergic receptors (GRIA1 and GRIA2) and cytoskeleton proteins (ACTB and ACTG) were more highly expressed in CA3. Altogether, these studies revealed that distinct hippocampal regions can be distinguished based on specific patterns of gene expression (Lein et al., 2004; Ginsberg and Che, 2005). These studies, however, did not identify the fundamental molecular and cellular characteristics that might make CA1 more vulnerable to pathology (Andersen et al., 2007).

[1] **Department of Psychiatry and Behavioral Sciences, UC Davis, Sacramento, California 95817;** [2] **The M.I.N.D. Institute, UC Davis, Sacramento, California 95817;** [3] **Department of Medicine, Unit of Physiology, University of Fribourg, 1700 Fribourg, Switzerland;** [4] **Department of Pathology, UC Davis, Sacramento, California 95817**

Additional Supporting Information may be found in the online version of this article.

Grant sponsor: Joe P. Tupin award, Department of Psychiatry and Behavioral Sciences; Grant sponsor: National Alliance for Research on Schizophrenia and Depression (NARSAD 2004 Young Investigator Award); Grant sponsor: Swiss National Science Foundation; Grant number: PP00A-106701; Grant sponsor: California National Primate Research Center; Grant number: RR00169.

*Correspondence to: Pierre Lavenex, Laboratory of Brain and Cognitive Development, Department of Medicine, Unit of Physiology, University of Fribourg, Chemin du Musée 5, CH-1700 Fribourg, Switzerland.
E-mail: pierre.lavenex@unifr.ch

In an effort to identify the molecular basis for the increased susceptibility of CA1 to hypoxia, we used genome-wide microarray analysis of gene expression to characterize the molecular signatures of five distinct regions of the rhesus monkey (*Macaca mulatta*) hippocampal formation [i.e., the entorhinal cortex (EC), the DG, CA3, CA1, and the subiculum] across four different postnatal ages (i.e., 1 day, 6 months, 1 yr, and 6–12 yrs of age). We performed Taqman® RT-PCR, immunohistochemistry and electron microscopy studies to corroborate and expand upon the microarray analyses. We found that a lower expression level of genes associated with astrocytic processes and functions characterizes the molecular signature distinguishing CA1 from other brain regions. Our findings suggest that the developmental decrease of astrocytic processes could underlie the selective vulnerability of CA1 during hypoxic-ischemic episodes in adulthood, its decreased susceptibility to febrile seizures with age, as well as contribute to the emergence of selective, adult-like memory function.

METHODS

Gene-Expression Analyses

Sixteen male rhesus monkeys (*Macaca mulatta*; four 1-day-olds, four 6-month-olds, four 1-yr-olds, and four 6–12-yrs-old adults) were used for this analysis. Monkeys were injected with an overdose of sodium pentobarbital (50 mg/kg i.v., Fatal-Plus, Vortech Pharmaceuticals, Dearborn, MI) and the brain rapidly extracted. Five-millimeter-thick slices of the brain were cut and stored overnight in RNAlater™ (Ambion, Austin, TX) at 4°C. Brain slices were then frozen in liquid nitrogen and resectioned at 100 μm for microdissection. Tissue samples included all layers of the EC at mid-rostrocaudal level (intermediate division, Ei), and all layers of the DG, CA3, CA1, and subiculum at mid-rostrocaudal level of the body of the hippocampus (at the level of the lateral geniculate nucleus). Only the mid-transverse portion of each region was dissected to ensure the specificity of the samples. The RNA sample from each region from each monkey was run on a separate chip, so that we had a total of four (animals per age) × four (ages) × five (regions) = 80 independent chips.

Microarray analysis was performed using the GeneChip® Human Genome U133 Plus 2.0 and the Two-Cycle Target Labeling and Control Reagents kit (Affymetrix, Santa Clara, CA) according to the manufacturer's protocol. Following the first round of amplification with the MEGAscript T7 Kit (Ambion) and synthesis of double stranded cDNA, a second round of in vitro transcription was carried out using the IVT labeling Kit (Affymetrix). U133 Plus 2.0 arrays were scanned on a GeneChip Scanner 3,000. Analyses of gene expression levels were performed with ArrayAssist® Expression Software 4.0 (Stratagene, La Jolla, CA).

Taqman® RT-PCR was performed for a subset of genes as described previously (Baron et al., 2006). Total RNA from the same samples used for the microarray experiments were used. We limited the Taqman® analyses to the three older groups (6-month, 1-yr, and adult monkeys), as RNA samples from newborn individuals were not available in sufficient amounts to run these analyses. The following Taqman® assays were used: glial fibrillary acidic protein (GFAP), Hs00157674_m1; SLC1A1, Hs00188172_m1; SLC1A3, Hs00904824_m1; ATP1A1, Hs00167556_m1; phosphoglycerate kinase (PGK1), Hs99999906_m1; GLUL, Hs00374213_m1; SLC1A2, Hs00188189_m1; glucose phosphate isomerase (GPI), Hs00164752_m1.

Immunohistochemical Analyses

The brains of 16 rhesus monkeys (four 1-day-olds [2M; 2F]; four 6-month-olds [2M; 2F]; four 1-yr-olds [2M; 2F], four adults [9–11-yrs-old; 2M; 2F]) were processed for the visualization of GFAP with a rabbit anti-GFAP polyclonal antibody (1:250; abcam ab16997, lot 495,288) following standard protocols (Lavenex et al., 2009). Digital pictures were taken with a Nikon Eclipse 80i equipped with an Optronics® (Goleta, CA) digital camera under standardized illumination conditions. All images were coded to allow blind analysis. Luminance measurements were taken on the acquired images with StereoInvestigator 7.0 (Microbrightfield, Williston, VT). A 75 × 75-μm frame was systematically, randomly placed across the different layers of CA3 and CA1. Luminance information for each frame was collected and normalized according to the following formula: luminance = (average luminance − [MAXi − MINi]). Average luminance is the average luminance in the RGB color space across the entire 75 × 75-μm field, MAXi is the luminance value for the individually brightest pixel in the field, and MINi is the luminance value for the individually dimmest pixel in the field. For CA3, strata oriens, pyramidale, lucidum, radiatum, and lacunosum moleculare were analyzed. For CA1, strata oriens, pyramidale, deep radiatum, superficial radiatum, and lacunosum moleculare were analyzed. Three independent measures were taken within each layer of each region, and the average value was calculated. Optical density data were then computed and normalized across all layers, regions, and animals according to the following formula: optical density = (100 − [(luminance + MINa)/(MAXa − MINa)] × 100]). Luminance corresponds to the value computed earlier, MINa is the minimum luminance value across all layers of the different regions from all animals, MAXa is the maximum luminance value across all layers of the different regions from all animals. Optical density values for CA1 and CA3 were computed, per animal, as the average of values for their different layers.

Electron Microscopy Analyses

We used the brains of twelve rhesus monkeys (six 1-day-olds [4 M, 2 F] and six adults [7.5–11-yrs-old; 4 M, 2 F]) collected in the context of other studies. Monkeys were deeply anesthetized with intravenous injection of sodium pentobarbital (50 mg/kg i.v., Fatal-Plus, Vortech Pharmaceuticals) and perfused transcardially with 4% paraformaldehyde (PFA) or 4% PFA + 0.5% glutaraldehyde in 0.1 M phosphate buffer (PB;

pH 7.4) following protocols previously described (Lavenex et al., 2009). The preparation of material followed standard electron microscopy protocols. Sections kept in TCS at −70°C were rinsed, postfixed in 1% glutaraldehyde, and embedded in Epon resin. Sections were examined with a light microscope and CA1 stratum radiatum was dissected, mounted on a resin block, serially sectioned into 70-nm-thick sections, and contrasted in Reynolds solution. Photomicrographs were taken as grayscale images at 46,000× magnification with a Philips CM100 transmission electron microscope, coded for blind analysis, and imported into Adobe Photoshop CS (version 8.0) at a resolution of 1,962 × 1,302 pixels (3,389 × 2,249 nm). Levels were adjusted manually, contrasts adjusted automatically, and images were saved as TIFF files at original resolution. Morphological measurements were performed with StereoInvestigator 7.0. A 1,000-nm-diameter circle was centered around a clearly defined synapse, and the following individual cellular components were identified and traced within this region: presynaptic neuronal component, postsynaptic neuronal component, astrocytic processes, and other neuronal processes that were not part of the examined synapse. Morphological criteria to identify astrocytic processes were previously described by Ventura and Harris (1999). The surface area occupied by these different cellular components was expressed as a percentage of the 1,000-nm-diameter circle. Ten synapses were evaluated per monkey and an average value was calculated for each monkey.

Statistical Analyses

Data are presented as group average and standard error of the mean. We performed analyses of variance (ANOVAs), with age as a factor and region as the repeated measure, to analyze gene expression and immunohistochemistry data, which were normally distributed. Mann–Whitney tests were performed to analyze electron microscopy data. Statview 5.0.1 statistical software was used for all statistical analyses (SAS Institute). Significance level was set at $P < 0.05$.

RESULTS

GFAP Gene Expression Is Lower in CA1

We used the GeneChip Human Genome U133 Plus 2.0 (Affymetrix) to analyze gene expression in five distinct hippocampal regions: the EC, the DG, CA3, CA1, and the subiculum. Probe-level analysis was performed with the Robust Multichip Averaging algorithm. Data were log 2 transformed, and an ANOVA was performed in order to identify genes with differential expression in any of the five hippocampal regions. Adjusted *P*-values for multiple comparisons were calculated with the false discovery rate method of Benjamini and Hochberg (1995). We found that an unusually large number of genes associated with astrocytes, glycolysis and glutamate metabolism exhibited a twofold lower level of expression in the CA1 field of the monkey hippocampus (Supporting Information 1), when compared with every other region analyzed. These genes included GFAP, apolipoprotein E (APOE), glyceraldehyde 3-phosphate dehydrogenase (GAPDH), PGK1, Na^+/K^+ ATPase (ATP1A1), and glutamine synthetase (GLUL). We further used Taqman® RT-PCR to evaluate the expression levels of eight genes involved in glutamate reuptake by astrocytes and neurons (Supporting Information 2). Consistent with the microarray data, Taqman® analysis indicated that seven of these genes exhibited lower expression levels in CA1 when compared with every other region: GFAP, SLC1A2 (EAAT2 = GLT-1, glutamate glial transporter), SLC1A3 (EAAT1 = GLAST, glutamate glial transporter), ATP1A1, PGK1, GLUL, and GPI. The genes SLC1A2, SLC1A3, and GPI were not present in the initial list of 108 genes with a lower expression level in CA1 (Supporting Informaion 1), because the cut-off was set at a fold change of two, and a statistical correction for mutliple comparisons (Benjamin and Hochberg, 2005) was applied to select that group of genes (statistical analyses performed on the microarray data derived from individual probes for these genes were consistent with the Taqman® RT-PCR data). In contrast, both microarray and Taqman® analyses indicated that the gene SLC1A1 (EAAC1 = EAAT3), which codes for the glutamate transporter expressed in neurons, was not differentially expressed in CA1 when compared with all the other regions. Thus, a lower expression level of genes associated with astrocytic processes and functions characterizes the molecular signature distinguishing CA1 from other brain regions.

Because hippocampus susceptibility to hypoxia increases with age (Kass and Lipton, 1989), we examined the regulation of gene expression in the hippocampus at different postnatal ages. We found that the genes with lower expression levels in CA1 generally exhibited distinct patterns of regulation in the CA1 and CA3 fields of the hippocampus during early postnatal development. We focus here on the GFAP gene (Fig. 1), a specific marker of astrocytes (Reichenback and Wolburg, 2005), which are of particular importance to understanding hippocampal vulnerability to hypoxic-ischemic insult. GFAP gene expression decreased between birth and 6 months of age in CA1 [$F(3,12) = 14.93$, $P = 0.0002$; newborn > 6-month = 1-yr = adult, all $P < 0.0005$], whereas it decreased between 1 yr of age and adulthood in CA3 [$F(3,12) = 26.07$, $P = 0.0001$; newborn = 6-month = 1-yr > adult, all $P < 0.0001$; ANOVA: age: $F(3,12) = 8.073$, $P = 0.0033$; region: $F(4,48) = 73.198$, $P = 0.0001$; interaction: $F(4,48) = 10.703$, $P = 0.0001$]. GFAP gene expression did not differ between CA1 and CA3 in newborn monkeys [paired *t*-test: $t(3) = 0.91$, $P = 0.4317$], but differed between CA1 and CA3 at other ages, including in adult monkeys [$t(3) = 5.07$, $P = 0.0148$]. A number of other genes associated with astrocytic processes and functions, such as APOE, GAPDH, GPI, ATP1A1, SLC1A2, and GLUL, exhibited similar developmental decreases in expression in CA1. Although these genes also exhibited a developmental decrease in expression in

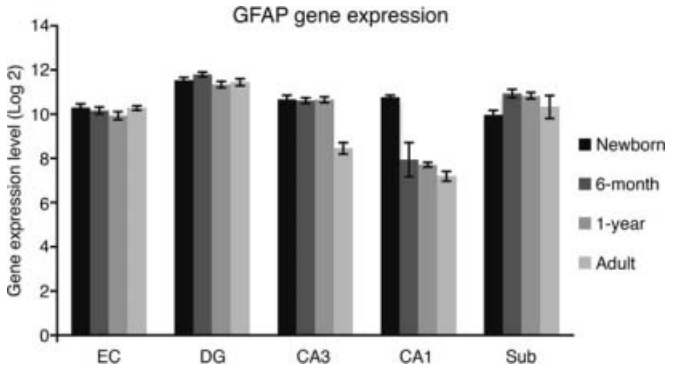

FIGURE 1. Microarray analysis: GFAP gene expression decreased between birth and 6 months of age in CA1. GFAP gene expression decreased between 1 yr of age and adulthood in CA3. GFAP gene expression did not differ between CA3 and CA1 at birth, but differed at all other ages. EC, entorhinal cortex; DG, dentate gyrus; CA3 and CA1, fields of the hippocampus; Sub, subiculum.

CA3, the decrease was always more pronounced in CA1, resulting in lower expression levels in the CA1 of adult individuals.

GFAP Protein Expression Is Lower in CA1

To confirm the microarray findings showing a developmental decrease in the expression of the GFAP gene, we evaluated the distribution of the GFAP using immunohistochemical techniques (Fig. 2). Optical density measurements revealed differential developmental decreases in GFAP immunostaining in CA1 and CA3 (Fig. 3; age $F(3,12) = 10.62$, $P = 0.001$; region $F(1,12) = 1221.53$, $P < 0.0001$; interaction $F(3,12) = 4.37$, $P = 0.0269$). In CA1, optical density was higher in newborns when compared with all other ages [$F(3,12) = 9.39$, $P = 0.0018$; newborn > 6-month = 1-yr > adult, all $P < 0.05$], whereas in CA3, optical density was lower in adults when compared with all other ages [$F(3,12) = 10.06$, $P = 0.0014$; newborn = 6-month = 1-yr > adult, all $P < 0.05$]. Although optical density did not differ between CA1 and CA3 in newborns [paired t-tests: $t(3) = 2.51$, $P = 0.0871$], it was lower in CA1 in 6-month-olds [$t(3) = 7.37$, $P = 0.0052$], 1-yr-olds [$t(3) = 9.58$, $P = 0.0024$] and adults [$t(3) = 4.39$, $P = 0.0219$]. Expression patterns of the GFAP thus paralleled the expression patterns observed at the RNA level.

Developmental Decrease of Astrocytes in CA1

To determine whether the developmental decreases in GFAP gene and protein expression were reflected at the synaptic level, we measured the surface area occupied by astrocytic processes surrounding excitatory synapses in the stratum radiatum of CA1 in newborn and adult monkeys. Stratum radiatum is the main termination zone for the dense network of excitatory projections arising from CA3 pyramidal neurons and reaching CA1, the so-called Schaffer collaterals. We found that, in newborns, astrocytic processes occupied 10.62% ± 0.55% of the surface area surrounding excitatory synapses, whereas, in adults, astrocytic processes occupied only 5.08% ± 0.88% of the surface area (Fig. 4; Mann–Whitney U; $Z = -2.88$, $P = 0.0039$). In contrast, the space occupied by neuronal elements that were not part of the synapse did not differ between newborns and adults (Mann–Whitney U; $Z = -1.28$, $P = 0.2002$) nor did the size of the presynaptic and postsynaptic elements (presyn: Mann–Whitney U; $Z = -1.28$, $P = 0.2002$; postsyn: Mann–Whitney U; $Z = -1.12$, $P = 0.2623$). These findings at the ultrastructural level confirm the observations at the RNA and protein levels and specifically demonstrate that the astrocytic coverage of excitatory synapses in the monkey CA1 stratum radiatum decreases during postnatal development.

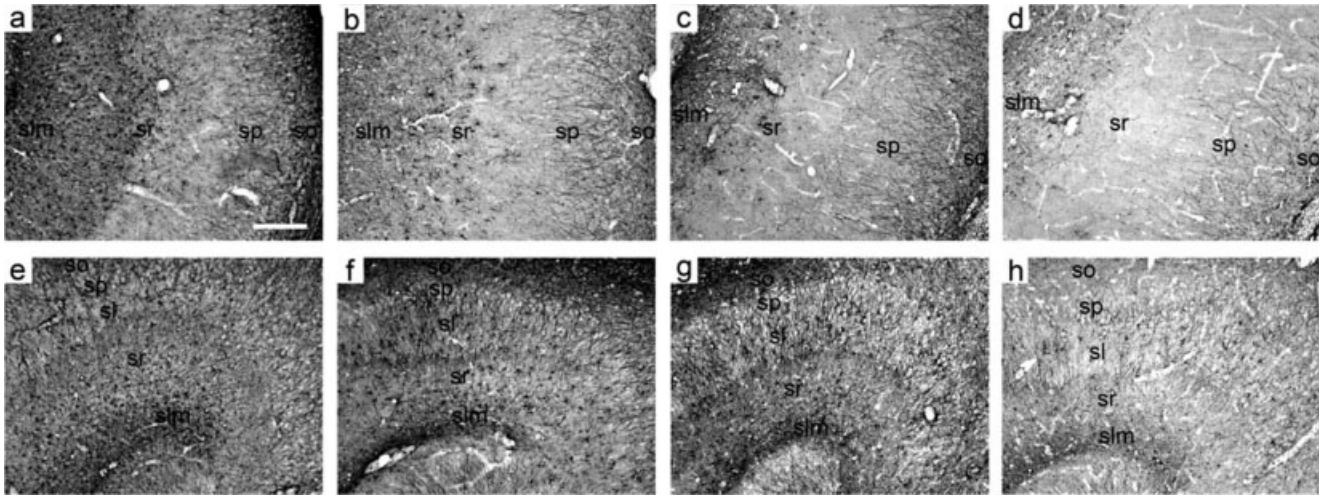

FIGURE 2. GFAP immunohistochemistry. (a) CA1 in a newborn monkey. (b) CA1 in a 6-month-old monkey. (c) CA1 in a 1-yr-old monkey. (d) CA1 in an adult monkey. (e) CA3 in a newborn monkey. (f) CA3 in a 6-month-old monkey. (g) CA3 in a 1-yr-old monkey. (h) CA3 in an adult monkey. Scale bar in a = 100 μm, applies to all panels. sl,: stratum lucidum; slm, stratum lacunosum-moleculare; so, stratum oriens; sp, stratum pyramidale; sr, stratum radiatum.

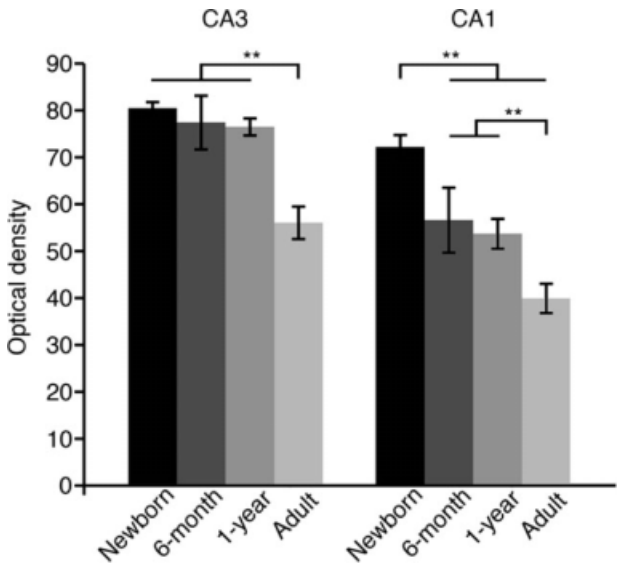

FIGURE 3. GFAP immunostaining decreased between birth and 6 months of age in CA1. GFAP immunostaining decreased between 1 yr of age and adulthood in CA3. GFAP immunostaining did not differ between CA3 and CA1 at birth, but differed at all other ages.

DISCUSSION

We used genome-wide microarray analysis of gene expression to characterize the molecular signatures of five distinct hippocampal regions across early postnatal development in monkeys. We found that a large number of genes associated with glycolysis and glutamate metabolism in astrocytes exhibited a lower expression level in CA1, when compared with other hippocampal regions. Immunohistochemical analyses of the distribution of GFAP revealed a differential developmental decrease of astrocytes in CA3 and CA1. Finally, electron microscopy analyses of the relationship between astrocytic processes and excitatory synapses in stratum radiatum of CA1 revealed a significant decrease in the glial coverage of the synapses between birth and adulthood. Given the known role of astrocytes in the regulation of glutamate uptake and release at excitatory synapses, our findings suggest that the developmental decrease of astrocytic processes in the hippocampus might contribute to its decreased susceptibility to febrile seizures with age, its increased sensitivity to hypoxic-ischemic episodes with age and the emergence of adult-like memory function.

Comparison with Previous Studies

Gene expression

Previous studies in 10- to 11-week-old C57BL/6 mice (Lein et al., 2004) and 62–92-yr-old humans (Ginsberg and Che, 2005) revealed a number of genes to be differentially expressed in the DG versus CA3 versus CA1. A re-analysis of our own dataset acquired from monkeys ranging from in 1 day to 12 yrs of age, considering CA3 versus CA1 (Ginsberg and Che, 2005), or DG versus CA3 versus CA1 (Lein et al., 2004), confirmed a number of these findings (see Supporting Information 3). Differences in tissue sampling (microdissection vs. single-cell analysis) or life-experience (10-week-old laboratory mice vs. 62–92-yr-old humans) can easily explain the discrepancies between these studies. However, these data also suggest that the expression pattern of a number of genes can be used to define the molecular signatures of distinct hippocampal regions across species and different postnatal stages.

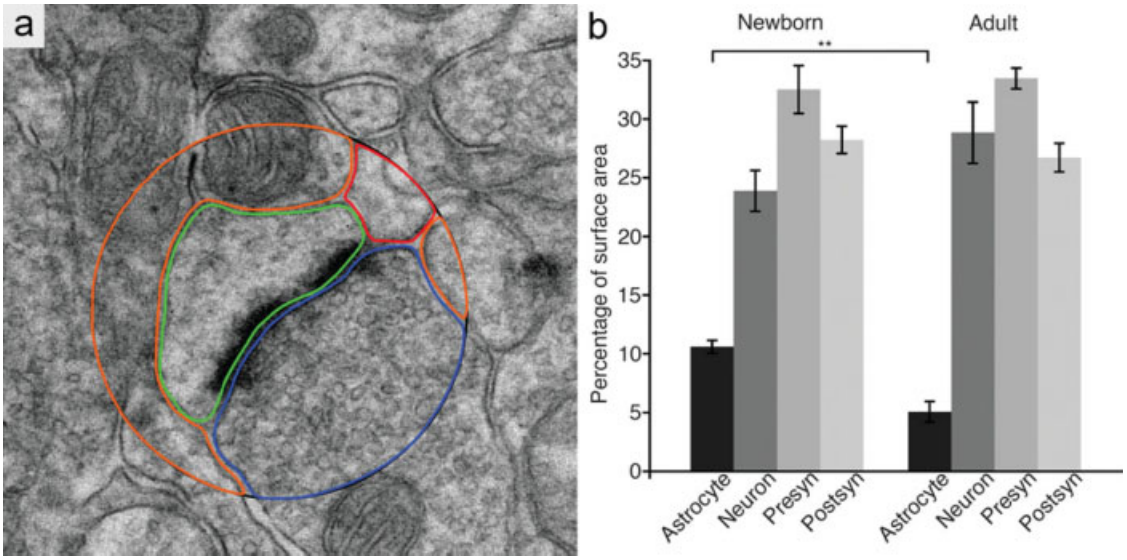

FIGURE 4. (a) Electron microscopy evaluation of astrocytic processes around excitatory synapses in the stratum radiatum of CA1. Blue outline: presynaptic neuronal element. Green outline: postsynaptic neuronal element. Orange outline: nonsynaptic neuronal elements. Red outline: astrocytic elements. Circle diameter: 1,000 nm. (b) The surface area occupied by astrocytic processes decreased between birth and adulthood. [Color figure can be viewed in the online issue, which is available at www.interscience.wiley.com.]

Immunohistochemistry

In the rat CA1, the density of GFAP-immunoreactive cells increases between 8 and 16 days of postnatal age, followed by a decrease in overall astrocyte size and number of terminal segments between 24 days and 2 months of age (Nixdorf-Bergweiler et al., 1994). Consistent with our findings in monkeys, 8–12-week-old male C57BL/6J mice also exhibit a higher numerical density of astrocytes in the dorsal CA3 stratum radiatum when compared with the dorsal CA1 stratum radiatum (Ogata and Kosaka, 2002). Together, these data indicate that the postnatal maturation of the hippocampus is characterized, in both rodents and primates, by a developmental decrease in astrocytic processes and a lower density of astrocytes in CA1 when compared with CA3 in mature subjects.

Electron microscopy

Our findings are in agreement with an elegant study of the three-dimensional relationships between astrocytic processes and excitatory synapses in 1- to 2-month-old rats (Ventura and Harris, 1999), which indicated that thin sheets of astrocytic processes occupy only about 5% of the neuropil in CA1 stratum radiatum. Our analyses performed in two-dimensional space also found that astrocytic processes occupy only 5.08% $\pm$ 0.88% of the surface area surrounding excitatory synapses in 7.5–11-yr-old monkeys. More importantly, however, we demonstrated a significant decrease in the glial coverage of the synapses between birth and adulthood in monkeys.

Functional Implications

Sensibility to hypoxia

The susceptibility of the brain to hypoxic-ischemic episodes increases during postnatal development (Kass and Lipton, 1989; Towfighi et al., 1997; Vannucci and Hagberg, 2004). Within the hippocampal formation, Kass and Lipton (1989) have shown that dentate granule cells and CA1 pyramidal neurons are more sensitive to anoxia in 110–120-day-old rats when compared with 30–40-day-old rats. Moreover, the CA1 field is much more susceptible to anoxic damage than the DG (Kass and Lipton, 1986, 1989). However, until now, the reasons why CA1 is especially sensitive to glutamate excitotoxicity have remained elusive (Sommer, 1880; Spielmeyer, 1925; Zola-Morgan et al., 1986; Kass and Lipton, 1989; Towfighi et al., 1997; Nedergaard and Dirnagl, 2005; Andersen et al., 2007). Hypoxia reduces glycolysis (Supporting Information 4a,b), which in turn leads to a decrease in ATP levels (Kass and Lipton, 1989; Pellerin and Magistretti, 1994). As a consequence, the sodium–potassium gradient necessary for the cotransport of glutamate from the synaptic cleft into astrocytes dissipates (Swanson, 2005). This reduces glutamate clearance from the synapse, increasing neuronal depolarization and the potential for neuronal death via excitotoxicity (Swanson, 2005). High-astrocytic coverage, as we have shown in the newborn, likely maintains sufficient glutamate reuptake to limit neuronal depolarization and excitotoxicity during mild to moderate hypoxic-ischemic events. In the adult, however, a lower expression level of genes associated with glycolysis or glutamate uptake and metabolism (Rao et al., 2001), as well as a lower astrocytic coverage of excitatory synapses in CA1, render the system more vulnerable to a reduction in oxygen concentration. Our findings at the gene, protein, and structural levels thus suggest that the developmental decrease in astrocytic processes and functions may be the critical factor underlying the selective vulnerability of CA1 to hypoxic-ischemic episodes in adulthood. They also provide an explanation for the relative resistance of this brain structure to hypoxia in the perinatal period, and, in particular, during the birth process. What, then, are the functional benefits that might derive from structural changes that put CA1 at particular risk during episodes of hypoxia in adulthood?

Emergence of ''selective'' memory function

One major benefit that might derive from decreased astrocytic coverage is the regulation of synaptic efficacy that leads to an increase in synaptic selectivity advantageous for learning (Supporting Information 4c; Karlsson and Frank, 2008). Indeed, reduction of glutamate clearance associated with a relative decrease in astrocytic processes in the vicinity of synapses has been shown to affect transmitter release through modulation of presynaptic metabotropic glutamate receptors (Oliet et al., 2001). Reduced glutamate clearance results in increased glutamate concentration in the extracellular space (Tanaka et al., 1997; Bergles and Jahr, 1998), which in turn increases the activation of presynaptic mGluRs (Scanziani et al., 1997), thus leading to a lower probability of glutamate release by the presynaptic terminal (Oliet et al., 2001). It has been shown that presynaptic inhibition can be overcome by high-frequency bursts of afferent synaptic potentials (Grover et al., 2009), thus serving as a high-pass filter increasing the signal-to-noise ratio for information transmitted through these synapses (Oliet et al., 2001). Thus, the decreased astrocytic coverage of excitatory synapses that we observed in the adult CA1 could serve to ensure that only the most salient information generates synaptic activity in the hippocampal circuits that contribute to learning and memory processes. A developmental decrease of astrocytic processes and functions may therefore contribute to the emergence of adult-like, selective memory function.

Febrile seizures early in life

Finally, the relatively high astrocytic coverage of the newborn synapses might also play a central role in the generation of febrile seizures. The highest incidence of seizures is in the first year of life in humans and is most often associated with a febrile illness (Hauser, 1994). Fever begins with the activation of immune response cells that produce interleukin-1 (Supporting Information 4d), which in turn increases prostaglandin E2 synthesis (Biddle, 2006). Prostaglandins act at the level of the hypothalamus to regulate body temperature and induce fever.

Interestingly, prostaglandins have also been shown to stimulate calcium-dependent glutamate release in astrocytes (Bezzi et al., 1998; Volterra and Meldolesi, 2005), which can induce abnormal prolonged depolarization with repetitive spiking in CA1 pyramidal neurons leading to seizures (Kang et al., 2005; Tian et al., 2005). Thus, the relatively high-astrocytic coverage of the dense network of CA1 excitatory synapses in the newborn (twice that of the adult) could explain why infants exhibit a higher incidence of febrile seizures. The decrease in the astrocytic coverage of hippocampal excitatory synapses with development would thus reduce the probability of neuronal depolarization evoked by astrocytic glutamate release. Such structural changes might therefore provide the cellular basis for the decreased susceptibility to febrile seizures with age.

CONCLUSION

Our study has identified structural characteristics that might provide the neurobiological basis for the selective vulnerability of the hippocampus to hypoxic-ischemic episodes in adulthood, the relative resistance of this brain region to hypoxia at birth, its susceptibility to febrile seizures within the first years of life, as well as explain the functional benefits that derive from structural changes that put CA1 at particular risk in case of hypoxia in adulthood.

Acknowledgments

We thank David G. Amaral for his support throughout the study, and Jane Favre and especially Danièle Uldry for technical assistance.

REFERENCES

Amaral DG, Lavenex P. 2007. Hippocampal neuroanatomy. In: Andersen P, Morris RGM, Amaral DG, Bliss TV, O'Keefe J, editors. The Hippocampus Book. Oxford: Oxford University Press. pp 37–114.

Andersen P, Morris RG, Amaral DG, Bliss TV, O'Keefe J. 2007. Historical perspective: Proposed functions, biological characteristics, and neurobiological models of the hippocampus. In: Andersen P, Morris RGM, Amaral DG, Bliss TV, O'Keefe J, editors. The Hipppocampus Book. Oxford: Oxford University Press. pp 9–36.

Banta Lavenex P, Amaral DG, Lavenex P. 2006. Hippocampal lesion prevents spatial relational learning in adult macaque monkeys. J Neurosci 26:4546–4558.

Baron CA, Tepper CG, Liu SY, Davis RR, Wang NJ, Schanen NC, Gregg JP. 2006. Genomic and functional profiling of duplicated chromosome 15 cell lines reveal regulatory alterations in UBE3A-associated ubiquitin-proteasome pathway processes. Hum Mol Genet 15:853–869.

Benjamini Y, Hochberg Y. 1995. Controlling the false discovery rate: A practical and powerful approach to multiple testing. JR Stat Soc B 57:289–300.

Bergles DE, Jahr CE. 1998. Glial contribution to glutamate uptake at Schaffer collateral-commissural synapses in the hippocampus. J Neurosci 18:7709–7716.

Bezzi P, Carmignoto G, Pasti L, Vesce S, Rossi D, Rizzini BL, Pozzan T, Volterra A. 1998. Prostaglandins stimulate calcium-dependent glutamate release in astrocytes. Nature 391:281–285.

Biddle C. 2006. The neurobiology of the human febrile response. AANA J 74:145–150.

Galeffi F, Sah R, Pond BB, George A, Schwartz-Bloom RD. 2004. Changes in intracellular chloride after oxygen-glucose deprivation of the adult hippocampal slice: Effect of diazepam. J Neurosci 24: 4478–4488.

Giffard RG, Xu L, Zhao H, Carrico W, Ouyang Y, Qiao Y, Sapolsky R, Steinberg G, Hu B, Yenari MA. 2004. Chaperones, protein aggregation, and brain protection from hypoxic/ischemic injury. J Exp Biol 207:3213–3220.

Ginsberg SD, Che SL. 2005. Expression profile analysis within the human hippocampus: Comparison of CA1 and CA3 pyramidal neurons. J Comp Neurol 487:107–118.

Grover LM, Kim E, Cooke JD, Holmes WR. 2009. LTP in hippocampal area CA1 is induced by burst stimulation over a broad frequency range centered around delta. Learn Mem 16:69–81.

Hauser WA. 1994. The prevalence and incidence of convulsive disorders in children. Epilepsia 35:S1–S6.

Holopainen IE. 2005. Organotypic hippocampal slice cultures: A model system to study basic cellular and molecular mechanisms of neuronal cell death, neuroprotection, and synaptic plasticity. Neurochem Res 30:1521–1528.

Jensen FE. 2002. The role of glutamate receptor maturation in perinatal seizures and brain injury. Int J Dev Neurosci 20:339–347.

Kang N, Xu J, Xu Q, Nedergaard M, Kang J. 2005. Astrocytic glutamate release-induced transient depolarization and epileptiform discharges in hippocampal CA1 pyramidal neurons. J Neurophysiol 94:4121–4130.

Karlsson MP, Frank LM. 2008. Network dynamics underlying the formation of sparse, informative representations in the hippocampus. J Neurosci 28:14271–14281.

Kass IS, Lipton P. 1986. Calcium and long-term transmission damage following anoxia in dentate gyrus and CA1 regions of the rat hippocampal slice. J Physiol 378:313–334.

Kass IS, Lipton P. 1989. Protection of hippocampal slices from young rats against anoxic transmission damage is due to better maintenance of ATP. J Physiol 413:1–11.

Krebs C, Fernandes HB, Sheldon C, Raymond LA, Baimbridge KG. 2003. Functional NMDA receptor subtype 2B is expressed in astrocytes after ischemia in vivo and anoxia in vitro. J Neurosci 23: 3364–3372.

Kuan CY, Schloemer AJ, Lu A, Burns KA, Weng WL, Williams MT, Strauss KI, Vorhees CV, Flavell RA, Davis RJ, Sharp FR, Rakic P. 2004. Hypoxia-ischemia induces DNA synthesis without cell proliferation in dying neurons in adult rodent brain. J Neurosci 24: 10763–10772.

Lavenex P, Banta Lavenex P, Bennett JL, Amaral DG. 2009. Postmortem changes in the neuroanatomical characteristics of the primate brain: Hippocampal formation. J Comp Neurol 512:27–51.

Lein ES, Zhao XY, Gage FH. 2004. Defining a molecular atlas of the hippocampus using DNA microarrays and high-throughput in situ hybridization. J Neurosci 24:3879–3889.

Milner B, Squire LR, Kandel ER. 1998. Cognitive neuroscience and the study of memory. Neuron 20:445–468.

Morris RGM. 2007. Theories of hippocampal function. In: Andersen P, Morris RGM, Amaral DG, Bliss TV, O'Keefe J, editors. The Hippocampus Book. Oxford: Oxford University Press. pp 581–713.

Nedergaard M, Dirnagl U. 2005. Role of glial cells in cerebral ischemia. Glia 50:281–286.

Nixdorf-Bergweiler BE, Albrecht D, Heinemann U. 1994. Developmental changes in the number, size, and orientation of GFAP-positive cells in the CA1 region of rat hippocampus. Glia 12: 180–195.

Ogata K, Kosaka T. 2002. Structural and quantitative analysis of astrocytes in the mouse hippocampus. Neuroscience 113:221–233.
Oliet SH, Piet R, Poulain DA. 2001. Control of glutamate clearance and synaptic efficacy by glial coverage of neurons. Science 292: 923–926.
Pearson T, Nuritova F, Caldwell D, Dale N, Frenguelli BG. 2001. A depletable pool of adenosine in area CA1 of the rat hippocampus. J Neurosci 21:2298–2307.
Pellerin L, Magistretti PJ. 1994. Glutamate uptake into astrocytes stimulates aerobic glycolysis—A mechanism coupling neuronal-activity to glucose-utilization. Proc Natl Acad Sci USA 91:10625–10629.
Rao VL, Dogan A, Todd KG, Bowen KK, Kim BT, Rothstein JD, Dempsey RJ. 2001. Antisense knockdown of the glial glutamate transporter GLT-1, but not the neuronal glutamate transporter EAAC1, exacerbates transient focal cerebral ischemia-induced neuronal damage in rat brain. J Neurosci 21:1876–1883.
Reichenback A, Wolburg H. 2005. Astrocytes and ependymal glia. In: Kettenmann H, Ransom BR, editors. Neuroglia. Oxford: Oxford University Press. pp 19–35.
Scanziani M, Slain PA, Vogt KE, Malenka RC, Nicoll RA. 1997. Use-dependent increases in glutamate concentration activate presynaptic metabotropic glutamate receptors. Nature 385:630–634.
Sommer W. 1880. Erkrankung des Ammonshorns als aetiologisches moment der epilepsie. Arch Psychiatr Nervenkr 10:631–675.
Spielmeyer W. 1925. Zur Pathogenese örtlich elektiver Gehirnveränderungen. Z Ges Neurol Psychiatr 99:756–776.
Stork CJ, Li YV. 2006. Intracellular zinc elevation measured with a "calcium-specific" indicator during ischemia and reperfusion in rat hippocampus: A question on calcium overload. J Neurosci 26: 10430–10437.
Swanson RA. 2005. Astrocyte neurotransmitter uptake. In: Kettenmann H, Ransom BR, editors. Neuroglia. Oxford: Oxford University Press. pp 346–354.
Tanaka K, Watase K, Manabe T, Yamada K, Watanabe M, Takahashi K, Iwama H, Nishikawa T, Ichihara N, Kikuchi T, Okuyama S, Kawashima N, Hori S, Takimoto M, Wada K. 1997. Epilepsy and exacerbation of brain injury in mice lacking the glutamate transporter GLT-1. Science 276:1699–1702.
Tian GF, Azmi H, Takano T, Xu Q, Peng W, Lin J, Oberheim N, Lou N, Wang X, Zielke HR, Kang J, Nedergaard M. 2005. An astrocytic basis of epilepsy. Nat Med 11:973–981.
Towfighi J, Mauger D, Vannucci RC, Vannucci SJ. 1997. Influence of age on the cerbral lesions in an immature rat model of cerebral hypoxia-ischemia: A light microscopic study. Dev Brain Res 100: 149–160.
Vannucci SJ, Hagberg H. 2004. Hypoxia-ischemia in the immature brain. J Exp Biol 207:3149–3154.
Ventura R, Harris KM. 1999. Three-dimensional relationships between hippocampal synapses and astrocytes. J Neurosci 19:6897–6906.
Volterra A, Meldolesi J. 2005. Astrocytes, from brain glue to communication elements: The revolution continues. Nat Rev Neurosci 6: 626–640.
Yin HZ, Sensi SL, Ogoshi F, Weiss JH. 2002. Blockade of Ca^{2+}-permeable AMPA/kainate channels decreases oxygen-glucose deprivation-induced Zn^{2+} accumulation and neuronal loss in hippocampal pyramidal neurons. J Neurosci 22:1273–1279.
Zola-Morgan S, Squire LR, Amaral DG. 1986. Human amnesia and the medial temporal region enduring memory impairment following a bilateral lesion limited to field CA1 of the hippocampus. J Neurosci 6:2950–2967.